PROTEINS 2005 (In Press)

Modeling Side Chains Using Molecular Dynamics Improve Recognition of Binding Region in CAPRI Targets

Carlos J. Camacho

Department of Computational Biology, University of Pittsburgh,

200 Lothrop St, Pittsburgh, PA 15261, USA.

*Corresponding author: ccamacho@pitt.edu

Keywords: docking; protein interactions; complex structure; binding mechanism; recognition.

Running title: Modeling anchor residues using MD

Abstract

The CAPRI-II experiment added an extra level of complexity to the problem of predicting protein-protein interactions by including 5 targets for which participants had to build or complete the 3D structure of either the receptor or ligand based on the structure of a close homolog. In this paper, we describe how modeling key side chains using molecular dynamics (MD) in explicit solvent improved the recognition of the binding region of a free energy based computational docking method. In particular, we show that MD is able to predict with relatively high accuracy the rotamer conformation of the anchor side chains important for molecular recognition as suggested by Rajamani[1] et al., 2004. As expected, the conformations are some of the most common rotamers for the given residue, while latch side chains that undergo induced fit upon binding are forced into less common conformations. Using these models as starting conformations in conjunction with the rigid-body docking server *ClusPro* and the flexible docking algorithm *SmoothDock*, we produced valuable predictions for 6 of the 9 targets in CAPRI-II, missing only the three targets that underwent significant structural rearrangements upon binding. We also show that our free energy based scoring function, consisting on the sum of van der Waals, Coulombic electrostatic with a distance-dependent dielectric, and desolvation free energy, successfully discriminates the native-like conformation of our submitted predictions. The latter emphasizes the critical role that thermodynamics plays on our methodology, and validates the generality of the algorithm to predict protein interactions.

INTRODUCTION

Rajamani[1] et al. (2004) and Kimura[2] et al. (2000) have argued that in solution side chains important for molecular recognition (referred to as anchors or keys, respectively) acquired conformations similar to those in which they are found buried in the bound crystal structure. Using this highly specific structural motif protein-protein recognition can occur in a relatively short time scale (a few nanoseconds) without a stringent structural rearrangement. The encounter of these anchor side chains with their anchoring grooves lead to the formation of a weakly bound native-like intermediate that triggers the induced fit process responsible for the formation of the high affinity complex.

This new view of the binding process has obvious consequences for homology modeling, particularly for modeling side chains. Namely, the analysis of the rotamer conformations that surface side chains acquired in solution prior to the encounter with its binding partner should provide important clues as to how to build them in a homology model. Contrary to other areas of structural biology where side chains conformations are not very important, in the field of protein-protein interactions side chains conformers are everything. One poorly modeled side chain could be the difference between detecting and missing a protein interaction. The Second Critical Assessment of PRotein Interactions (CAPRI-II) provided excellent examples of this. In fact, in five of the initial targets of CAPRI-II participants were required to model the side chains of either the receptor or the ligand structure. For four of the target structures, homology modeling of the true target sequence was required since there was no crystal structure of the protein in question.

Besides a good model structure, detecting protein interactions require of an appropriate scoring function to identify the native complex. *In vitro* this scoring function is, of

course, the free energy. One of the main goals of CAPRI is to validate scoring functions.[3] In this regard, the automated server *ClusPro*[4] (http://structure.pitt.edu) was successful in predicting native-like models for 5 out of 10 targets based solely on thermodynamic free energy estimates.

The rigid-body docking server implements an electrostatic and desolvation free energy filtering,[5] and a clustering and ranking algorithm[6] of a homogenous sampling of the lowest free energy docked structures on the protein-protein interface. The initial screening of protein-protein encounter complexes is done using technologies that implement the breakthrough approach of Katchalski-Katzir and collaborators[7] that applies Fast Fourier Transform techniques to optimize a surface complementarity scoring function ---mostly the software DOT,[8] and ZDOCK.[9] The top clusters ranked by *ClusPro* are further optimized by smoothly adding the van der Waals interaction to our free energy function,[10] and then the optimized structures are re-ranked by the *SmothDock* algorithm.[6]

In this report, we show that modeling side chains based on the rotamer conformations sampled during a molecular dynamics (MD) simulation in explicit solvent of the isolated proteins improves recognition by refining key side chains into conformations amenable for rigid body docking. Excluding from our analysis those targets where the bound and unbound structure differed by more than 5Å, the method predicted very good (***) and good (**) models for all targets except for one that we only predicted acceptable models (*) according to the CAPRI assessors (Mendez and Wodak, this issue of Proteins). Our methods are highly automated and the main discrimination procedure is based on an empirical estimate of the binding free energy. Remarkably, our scoring function successfully identifies the native-like structures as those with the lowest free energy.

MATERIALS AND METHODS

Receptor-Ligand Protein Structures

The structures and templates for homology modeling were selected by the management committee of CAPRI. The proteins were quite diverse in structure and function. They included two antibody/antigen complexes, a homodimer, a homotrimer, three xylanase-xylanase inhibitors, a phosphotase and a regulatory subunit, among others.

Homology modeling

Four of the initially 12 targets of CAPRI2 corresponded to homology models. In all these cases, the best templates and alignments were given to the CAPRI participants. A fifth target included only the backbones of both receptor and ligand, thus modeling of side chains was required. All the models were built using the server *Consensus*,[11] which given a template construct the 3D structure including side chains by relying only in the structure of the template. *Consensus* also produces high quality alignment, but for these targets we only confirmed that the alignments provided by the CAPRI management were appropriate. Structures were then completed manually and minimized using CHARMm,[12] missing side chains were also built by CHARMm.

Side chain prediction using molecular dynamics

Once we have a full model of the protein structure, we solvate individual proteins in explicit water and perform standard molecular dynamics (MD) simulations using the program GROMACS[13] and default settings. Due to time constraints, in CAPRI we run very short MD. They were 300 μs long and harmonically constrained backbones,

dropping the first 100 μs as equilibration time. Then, we clustered the MD snapshots obtaining the most recurrent rotamer conformations, and we used those rotamers as side chain predictions. For the analysis presented here, we run 1.2 ns simulations, dropping the first 200 μs as equilibration time. No constrained was used on the protein backbones.

Prediction of docked conformations

The general procedure used to predict docked conformations has been described earlier.[6] The only biochemical information used was in Target 14,[14] where we found a description of the recognition binding site of the regulatory subunit by the protein phosphatase 1.[15] Otherwise, all our models were generated by refining the cluster structures predicted by the server *ClusPro*. It is important to emphasize that the free energy estimates used by our methods are not optimized using bound crystal structures but they are general empirical estimates of binding energies. The electrostatic potential is the standard Coulombic potential with a distance dependent dielectric of *4r*, and both polar and non-polar desolvation free energy including side chain entropy loss is estimated using a knowledge-based contact potential.[16,17] The van der Waals (VDW) energy is computed using CHARMm with CHARMm19 parameters.

RESULTS

Cohesin/Dockerin recognition mechanism (Targets 11 and 12)

Anchor side chains (i.e., side chains important for recognition) can be readily identified based on the crystal structure of the complex. Namely, they correspond to solvent exposed side chains that become buried upon binding, yielding the largest change in solvent accessible surface area.[1] For Target 11,[18] there are two anchor side chains, Leu83

in cohesin and Leu22 in dockerin, each burying 98 and 111 $Å^2$ of solvent accessible surface area[19] upon binding, respectively. The theory predicts that these two residues should be in bound-like rotamer conformation prior to the formation of an encounter complex.

In Fig. 1A, we show Leu22 in the bound (blue), in the template (cyan), and as in the model built for this target (red). For Target 11, the first homology modeling target of the CAPRI experiment, we built a full model of the dockerin molecule based on an NMR solution of a homolog (PDB code 1DAQ) using the method described in the Method section. Side chains were predicted by performing MD simulations of the protein in explicit solvent, and extracting the most representative rotamer conformations from the MD. As expected, the MD resulted in a Leu22 that was almost identical to the one in the bound complex. Unfortunately, the backbone of the homology model was poorly model (5Å away from the bound structure), so we failed to make a good prediction of the complex.

Let us then examine Target 12, as shown in Fig. 1B, the anchor Leu83 in Cohesin has very different conformations in the unbound (PDB code 1ANU) and the bound (1OHZ) structures.[18] In the bound crystal, the Leu22 and Leu83 snugly fit next to each other. In the unbound conformation, Leu83 (in red) blocks the cavity where Leu22 is supposed to anchor. Using the unbound structure of Cohesin, we predicted one of the best complex structures for Target 12 (shown in Fig. 1D). However, the rank of the prediction was not very good. The server *ClusPro* ranked this prediction Nr. 9, whereas *SmoothDock* re-ranked it to Nr. 8. As shown in Fig. 1D, the leucines clashed against each other when docking using the unbound Cohesin structure. Not surprisingly, our Nr. 1 prediction

shown in Fig. 1C has Leu22 docking on the opposite side of Leu83. The Dockerin structure possesses near perfect two-fold symmetry, and our model is basically rotated 180^{o} around Leu83. Interestingly, Fig. 1C is very close to most of the Nr. 1 predictions submitted for this target probably because most predictors docked using Leu83 as in 1ANU, the unbound structure of Cohesin.

Our hypothesis is that anchor side chains should dock relatively freely into their binding grooves, and Fig. 1B shows that this will not be the case for the unbound form of cohesin. This means that 1ANU should not be the conformation expected *in vitro*. In Fig. 2A, we show results from the MD simulations of (1ANU) cohesin, i.e. the RMSD of Leu83 with respect to its bound and unbound rotamer conformation as a function of time. Each point in the graph corresponds to a snapshot of the MD simulation. Based on Fig. 2A, we confirmed our hypothesis regarding anchor residues. Namely, MD clearly shows that for most of the time (60% or more) the visible rotamer conformation of Leu83 is within a few tenths of an Å from the bound rotamer. To confirm that this side chain is important for recognition, we re-submitted Target 11 to *ClusPro* using the same parameters as the ones used for CAPRI, but with Leu83 extracted from the MD. This time *ClusPro* completely reversed the ranking, the native-like prediction shown in Fig. 1D is now Nr. 1, and the "false-positive" shown in Fig. 1C is Nr. 9.

The detailed analysis of the mechanism of recognition of the Dockerin/Cohesin complex might also rationalize intriguing mutagenesis experiments that have shown that independently of each other the Dockerin duplets Ser45-Thr46 and Ser11-Thr12 are involved in a binding interaction.[18,20] While the crystal confirms that only Ser45-Thr46 is making an interaction with cohesin, it is perfectly feasible that blocking these residues (as

done experimentally) might trigger an interaction by the competing model shown in Fig. 1C that involves the second duplet Ser11-Thr12. The MD of Leu83 leaves this option open since this side chain moves back and forth between the bound and unbound state. In the unbound state, which is somewhat less likely than the bound state, the symmetric binding mode in Fig. 1C is preferred.

Ovine Prion (NMR)/Fab (bound) complex (Target 19)

Based on the crystal structure of this target 1TPX,[21] we identified the anchor residues of this complex as Val192 and Thr196 in the prion molecule, each burying 78 and 74 $Å^2$ of solvent accessible surface area, respectively. They also have a significant contribution to the binding free energy. Consistent with most antibody-antigen systems, the anchors bury a relatively small area.[1] A full atom MD of the prion molecule again confirms the prediction that these two side chains move closer to the bound rotamer and away from the original unbound conformation (see Fig. 2B and 2C). Because these side chains are relatively small, and even in the unbound structure (1DWY) they do not differ much from the bound rotamers, the improvement on the predictions by *ClusPro* after modeling the side chains according to the MD simulations was not as striking as for Target 12. It is interesting to note that the native-like rotamers acquired by these two side chains correspond to the most common rotamers in the rotamer table in Ref. 22.

Other homology modeling targets (Targets 16 and 17)

The same approach could be used to analyze the other homology model targets. However, the bound and unbound side chains for Target 16 and 17 (which were cancelled) were structurally very close to each other. In particular, the similarities between 1OM0 and the bound conformation of the XIP-I inhibitor for both targets 16 and

17 is remarkable. Of course, the two binding surfaces of XIP-I are relatively rigid. For Target 16, the anchor is Tyr238 does not change much between the bound and unbound conformation. Its chi1/chi2 rotamer angles are -69^o/98^o and -77^o/114^o in 1OM0 and in the complex 1TA3, respectively. This conformation of the Tyr side chain is the most common (45%) in protein structures.[22] The side chain of Lys234 acts as a latch of the native-like encounter complex and has room to rearrange after the native-like encounter complex is formed. In the unbound structure, one finds Lys234 in the "tttt" rotamer conformation, whereas in the bound structure it is in the relatively rare "pttp" rotamer conformation.[22] For Target 17, we run MD on the Xylanase. The anchor Asn123 is bound-like, whereas Arg149 (in XIP-1) is an important residue that retains the freedom to rearrange after the encounter complex is formed. Thus, Arg149 is a latch whose actual position prior to docking is less restricted than that of anchor residues. The submitted prediction for this target was acceptable and ranked Nr. 1.[23]

Free Energy discrimination of predictions submitted by Camacho

To show the robustness of our approach to protein docking, we show the total of the free energy function optimized by *SmoothDock*. The free energies plotted in Fig. 3 are computed by uploading our predictions from the CAPRI website and computing the sum of the VDW energy after 3 rounds of 20 standard minimization steps using CHARMm, plus the *4r* electrostatics and desolvation free energy terms. Since our electrostatic and desolvation scoring function is easily accessible to any reader in Ref. 17, Fig. 3 is straightforward to compute.

The models that the CAPRI assessors (Mendez and Wodak, this issue of Proteins) considered to be of the highest quality are marked by a red symbol. The assessors use a

Michelin ranking system of "***", "**", and "*" for models of High, Good, and Acceptable quality, respectively. In all cases, a top model (in red) had the lowest free energy of all submissions. The exception of Target 14 is only accidental, since our ** submission is almost identical to our acceptable * star models (8 of them). For Targets 8,[24] 13,[25] 14 and 19, our submissions ranked Nr. 1 are also found to have low free energy, and were assessed of high or acceptable quality by the assessors.

For Targets 12 and 18,[26] we predicted high quality models that are perfectly discriminated as the lowest free energy structures. Both of them, however, were ranked 8th. For Target 12, *SmoothDock*, a flexible side chain refinement procedure, predicted Fig. 1C as the top model. However, after *SmoothDock* set the ranking of the submissions, we replaced the bound side chains of the ligand back into our models. It turns out that the CHARMm minimization forced Leu83 to move out of the Leu22 pocket, building a better complex. Unfortunately, we only re-scored our predictions for the CAPRI meeting. Something similar occurred for Target 18, here we optimized the complex having a deprotonated His374 in the TAXI xylanase inhibitor. However, the association of TAXI and Xylanase (A. niger) is only possible with a protonated His374. The ranking shown in Fig. 3 was done using the protonated form of His374; in this condition the correct bound structure is ranked Nr. 1.

DISCUSSION

It is well known that a few side chains play a critical role in molecular recognition. The results shown here provide further insights as to how they enhance or hinder molecular recognition. In the case of the Cohesin/Dockerin interaction, Leu83 switches between an *on* and *off* conformation in time scales on the order of a tenth of a nanosecond. This time

scale should be compared with the lifetime of an encounter complex, i.e. a few nanoseconds. The suggested scenario is that as Dockerin and Cohesin approach to close proximity, Leu22 has enough time for Leu83 to display the attractive groove where it should anchor. We also show that if Leu83 is in the *off* position (as in the unbound structure) a competing interaction is observed, where instead of Ser45 and Thr46 making important contacts, one finds the symmetric residues Ser11 and Thr12 making the contacts. This prediction could in fact be checked experimentally, preliminary evidence already indicates that a competing binding mode involving Ser11 and Thr12 exists.

A comparison of rotamer conformations between those found in the crystal structures or extracted from MD simulations and those from rotamer tables[22] show that anchor residues are often found in some of the most likely side chain rotamer conformations. This is consistent with the expectation that these residues do not change conformation upon binding. On the other hand, side chains that undergo induced fit, referred to as latches, are found in relatively unlikely rotamers. The latter is consistent with the greater role played by the local environment in inducing structural rearrangements of latch side chains.

We validated our free energy scoring function by showing that a native-like model had always the lowest binding free energy. It is important to emphasize that our scoring function should not work for submissions from other groups. Since, as far as we know, we are the only group that optimizes the VDW energy as part of our refinement procedure.

As in CAPRI-I, the only targets that we predicted successfully were those for which *ClusPro* was able to rank a native-like cluster within the top 25 predictions. Given such a

cluster, our *SmoothDock* refinement algorithm was able to re-rank the predictions within the top submissions. The only Targets that we failed to submit a good prediction were those for which there was a significant difference between the bound and unbound structures.

CONCLUSION

We have shown some examples that describe in detail how the dynamics of anchor side chains is critical for molecular recognition. Our algorithms consistently identify a native-like complex of two interacting proteins that do not undergo a significant rearrangement upon binding. Together with the success shown by *ClusPro* that predicted 5 targets without the use of any literature information,[22] we show that our free energy scoring function is robust and general enough to discriminate true from false positives. It would be interesting to know whether any other group validated their scoring function as we did in Fig. 3, or if the ranking of complex structures is mostly based on literature information and human intuition.

ACKNOWLEDGEMENTS

The models submitted to CAPRI (3/2004) were made while CJC was a Faculty member of the Department of Biomedical Engineering at Boston University supported by NIH Grant GM061867. The analysis presented in this report was supported by the University of Pittsburgh. The author is grateful to the referee for suggesting a comparison with data from a rotamer table, J.C. Prasad for building the initial homology models, S. Thiel for running the MD simulations that were used in CAPRI, and specially S.R. Comeau for running the server *ClusPro*.

REFERENCES

1. Rajamani D, Thiel S, Vajda S, Camacho CJ. Anchor residues in protein-protein interactions. Proc. Natl. Acad. Sci. USA 2004;101:11287-11292.

2. Kimura SR, Brower RC, Vajda S, Camacho CJ. Dynamical view of the positions of key side chains in protein-protein recognition. Biophys. J. 2001;80:635-642.

3. Janin J, Henrick K, Moult J, Ten Eyck L, Sternberg MJ, Vajda S, Vakser I, Wodak SJ. CAPRI: A Critical Assessment of PRedicted Interactions. Proteins 2003;52:2-9.

4. Comeau SR, Gatchell DW, Vajda S, Camacho CJ. *ClusPro*: an automated docking and discrimination method for the prediction of protein complexes. Bioinformatics 2004;20:45-50.

5. Camacho CJ, Gatchell DW, Kimura SR, Vajda S. Scoring docked conformations generated by rigid-body protein-protein docking. Proteins 2000;40:525 – 537.

6. Camacho CJ, Gatchell DW. Successful discrimination of protein interactions. Proteins 2003;52:92-97.

7. Katchalski-Katzir E, Shariv I, Eisenstein M, Friesem A, Aflalo C, Vakser IA. Molecular surface recognition - determination of geometric fit between proteins and their ligands by correlation techniques. Proc. Natl. Acad. Sci., USA 1992;89:2195-2199.

8. Ten Eyck LF, Mandell J, Roberts VA, Pique ME. Surveying molecular interactions with DOT. In Proceedings of the 1995 ACM/IEEE Supercomputing Conference. (ed. Hayes, A. and Simmons, M.) , ACM Press, New York.

9. Chen R, Li L, Weng Z. ZDOCK: an initial-stage protein docking algorithm. Proteins 2003;52:82-87.

10. Camacho CJ, Vajda S. Protein docking along smooth association pathways. Proc. Natl. Acad. Sci., USA 2001;98:10636-10641.

11. Prasad JC, Comeau SR, Vajda S, Camacho CJ. Consensus alignment for reliable framework prediction in homology modeling. Bioinformatics 2003;19:1682-1691.

12. Brooks BR, Bruccoleri RE, Olafson BD, States DJ, Swaminathan S, Karplus M. CHARMm: A program for macromolecular energy, minimization, and dynamics calculations. J. Comput. Chem. 1983;4:187-217.

13. Lindahl E, Hess B, van der Spoel D. GROMACS 3.0: A package for molecular simulation and trajectory analysis (2001) J. Mol. Mod. 2001;7:302-317.

14. Terrak M, Kerff F, Langsetmo K, Tao T, Dominguez R. Structural basis of protein phosphatase 1 regulation. Nature 2004;429:780-784.

15. Egloff MP, Johnson DF, Moorhead G, Cohen PTW, Cohen P, Barford D. Structural basis for the recognition of regulatory subunits by the catalytic subunit of protein phosphatase 1. EMBO J. 1997;16:1876-1887.

16. Zhang C, Vasmatzis G, Cornette JL, DeLisi, C. Determination of atomic desolvation energies from the structures of crystallized proteins. J. Mol. Biol. 1997;267: 707–726.

17. Camacho CJ, Zhang C. *FastContact*: Rapid Estimate of Contact and Binding Free Energies. Bioinformatics 2005; In press.

18. Carvalho AL, Dias FM, Prates JA, Nagy T, Gilbert HJ, Davies GJ, Ferreira LM, Romao MJ, Fontes CM. Cellulosome assembly revealed by the crystal structure of the cohesin-dockerin complex. Proc. Natl. Acad. Sci. USA 2003;100:13809-13814.

19. Lee B, Richards FM. The interpretation of protein structures: estimation of static accessibility. J. Mol. Biol. 1971;55:379-400.

20. Schaeffer F, Matuschek M, Guglielmi G, Miras I, Alzari PM, Beguin P. Duplicated dockerin subdomains of Clostridium thermocellum endoglucanase CelD bind to a cohesin domain of the scaffolding protein CipA with distinct thermodynamic parameters and a negative cooperativity. Biochemistry 2002;39:5013-5021.

21. Eghiaian F, Grosclaude J, Lesceu S, Debey P, Doublet B, Treguer E, Rezaei H, Knossow M. Insight into the PrPC-->PrPSc conversion from the structures of antibody-bound ovine prion scrapie-susceptibility variants. Proc. Natl. Acad. Sci. USA 2004;101:10254-10259.

22. Lovell SC, Word JM, Richardson JS, Richardson DC. The penultimate rotamer table. Proteins 2000;40:389-408.

23. Comeau SR, Vajda S, Camacho CJ. Performance of the First Protein Docking Server *ClusPro* in CAPRI Rounds 3-5. Proteins 2005; this issue.

24. Takagi J, Yang Y, Liu JH, Wang JH, Springer TA. Complex between nidogen and laminin fragments reveals a paradigmatic beta-propeller interface. Nature 2003;424:969-974.

25. Graille M, Stura E, Bossus M, Muller BH, Letourneur O, Battail-Poirot N, Sibaï G, Gauthier M, Rolland D, Le Du MH, Ducancel F. Structure of the immunodominant epitope displayed by the surface antigen 1 (SAG1) of *Toxoplasma gondii* complexed to a monoclonal antibody. (Submitted)

26. Sansen S, De Ranter CJ, Gebruers K, Brijs K, Courtin CM, Delcour JA, Rabijns A.

Structural basis for inhibition of Aspergillus niger xylanase by triticum aestivum xylanase inhibitor-I. J. Biol. Chem. 2004;279:36022-36028.

FIGURE CAPTIONS

Figure 1: Analysis of anchor side chains on the Cohesin/Dockerin complex. (A) Dockerin structure in the complex structure (blue), in the NMR homolog 1DAQ (cyan), and in the homology model used for Target 11 (red). The anchor side chain Leu22, modeled following a short MD in explicit solvent, is almost the same as the one seen in the bound structure. This conformation is also similar to the most common Leu rotamer observed in crystal structures, i.e., the "mt" rotamer in Lovell et al. rotamer table.[22] (B) Bound (blue) and unbound (red) form of the receptor Cohesin, and side chain of Leu83. (C) Prediction ranked Nr. 1 both by the server *ClusPro* and by the *SmoothDock* algorithm. Both methods docked Dockerin against the unbound form of Cohesin with Leu83 in the "wrong" rotamer conformation (in red). (D) The bound ligand is shown in blue. The native-like predictions of *ClusPro* ranked 9^{th} and *SmoothDock* ranked 8^{th} are in red. This model is ranked Nr. 1 if *ClusPro* is run using the bound side chain of Leu83 shown in blue.

Figure 2: RMSD of side chains with respect to the bound (blue) and unbound (red) side chain as a function of time. The data is from snapshots of a 1.2 ns MD in explicit solvent that are overlapped to the bound and unbound chain (see text). (A) For Leu83 in Cohesin (Target 11 and 12), the bound rotamer (chi1/chi2 equal to $173^o/62^o$) is close to the second most common Leu rotamer (chi1/chi2 equal to $177^o/63^o$ in Ref. 22), while the unbound rotamer corresponds to a very infrequent conformation (chi1/chi2 equal to $-64^o/100^o$ in

1ANU, and around -79^{o}/54^{o} in the MD) similar to rotamer “mp” (-85^{o}/65^{o}) in Ref. 22. Anchors (B) Val192 and (C) Thr196 from the Prion molecule in Target 19, both showing a consistent trend towards native-like rotamers.

Figure 3: Free energy as a function of ligand RMSD for the 6 CAPRI targets that did not change much between the bound and unbound structure. Symbols in red correspond to all the highest score models for each target. The number next to the symbol indicates the ranking of the model, and the stars correspond to the assessment given to the model by CAPRI assessors.

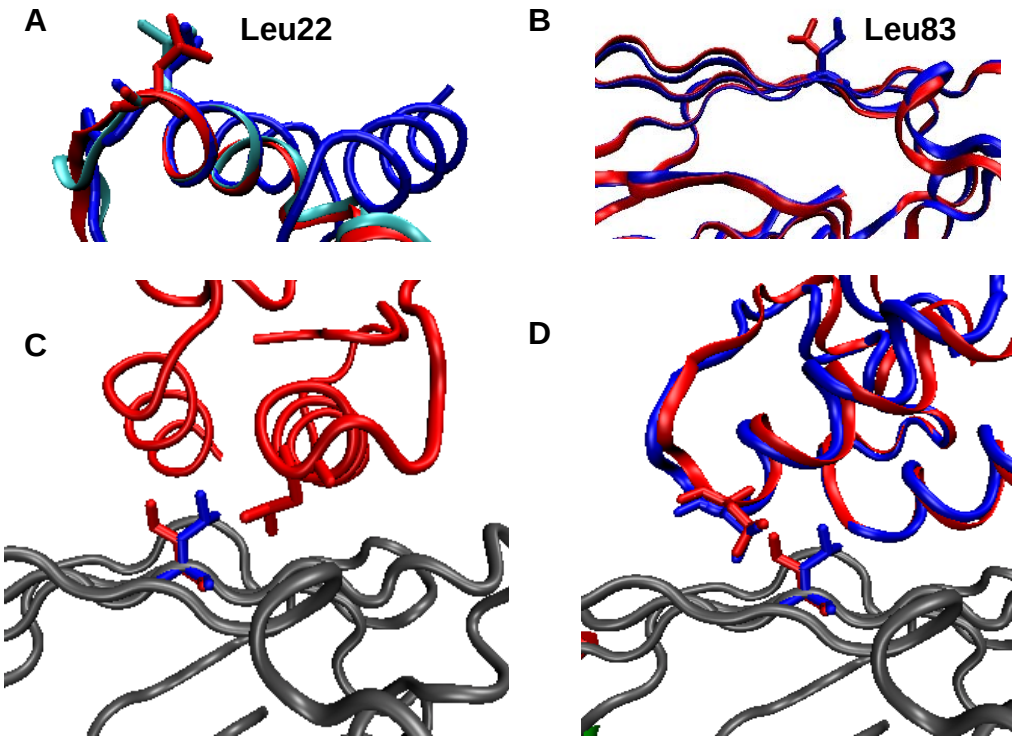

FIGURE 1

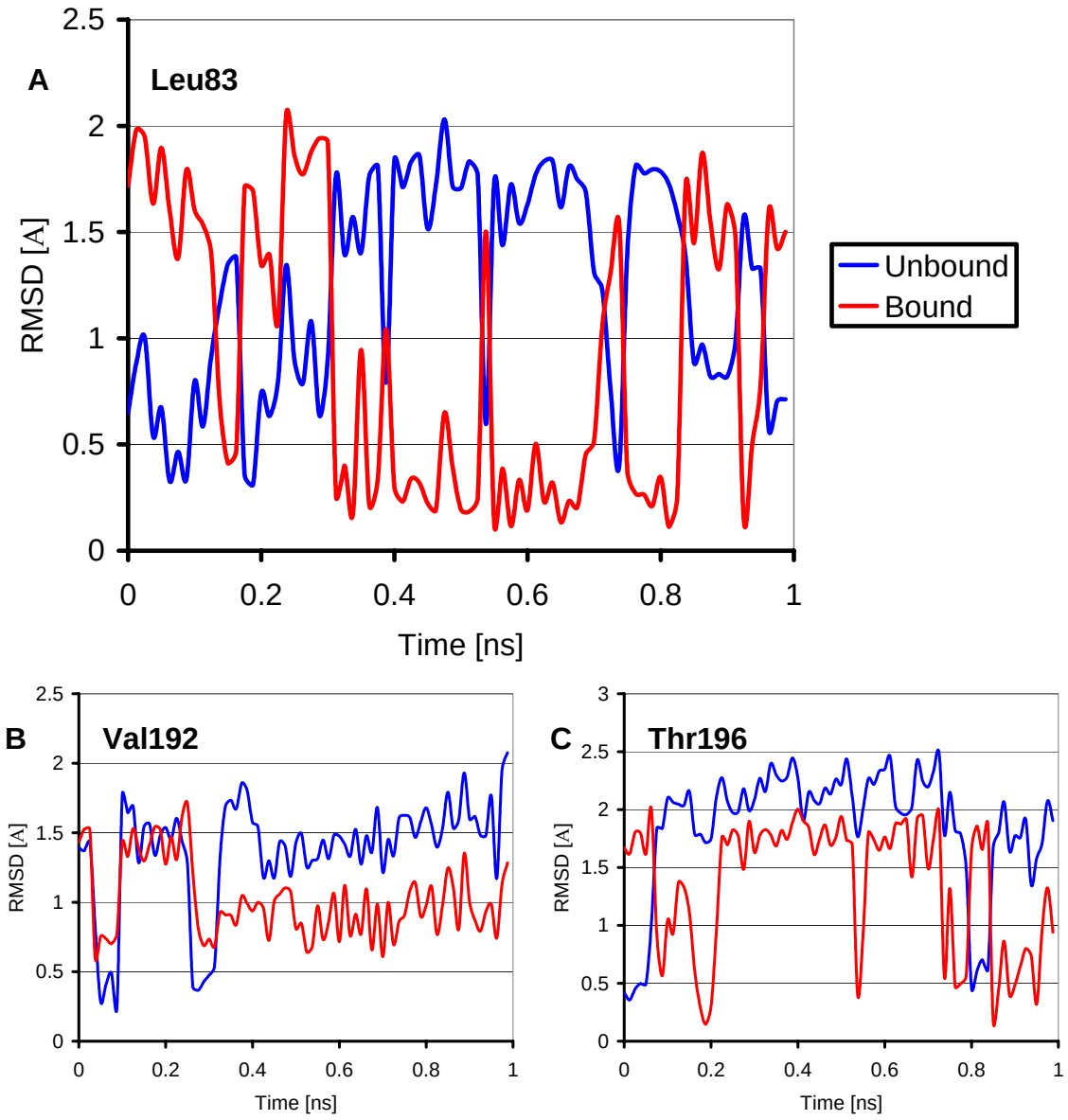

FIGURE 2

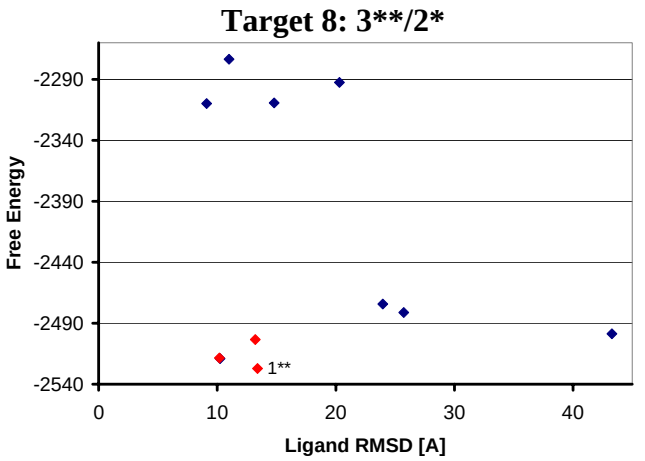
Target 8: 3**/2*
Free Energy
-2290
-2340
-2390
-2440
-2490
-2540
0
10
20
30
40
1**
Ligand RMSD [A]

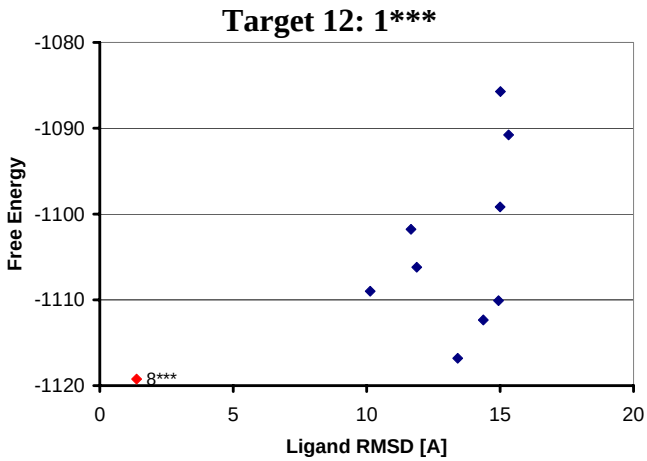
Target 12: 1***
Free Energy
-1080
-1090
-1100
-1110
-1120
0
5
10
15
20
8***
Ligand RMSD [A]

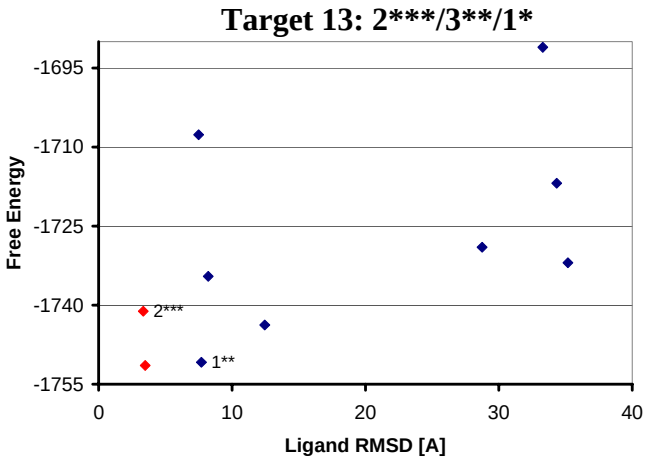
Target 13: 2***/3**/1*
Free Energy
-1695
-1710
-1725
-1740
-1755
0
10
20
30
40
2***
1**
Ligand RMSD [A]

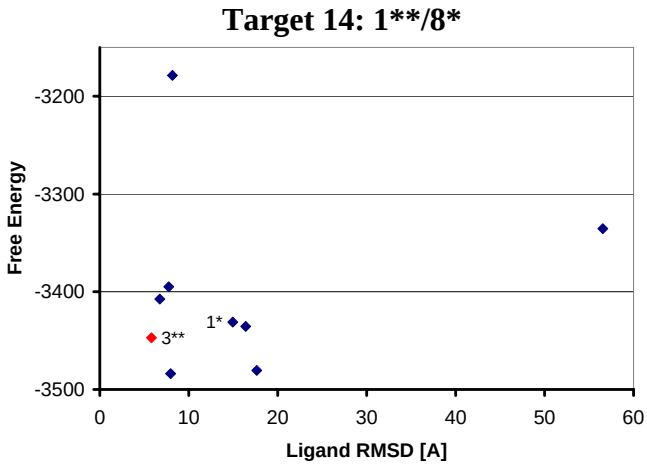
Target 14: 1**/8*
Free Energy
-3200
-3300
-3400
-3500
0
10
20
30
40
50
60
1*
3**
Ligand RMSD [A]

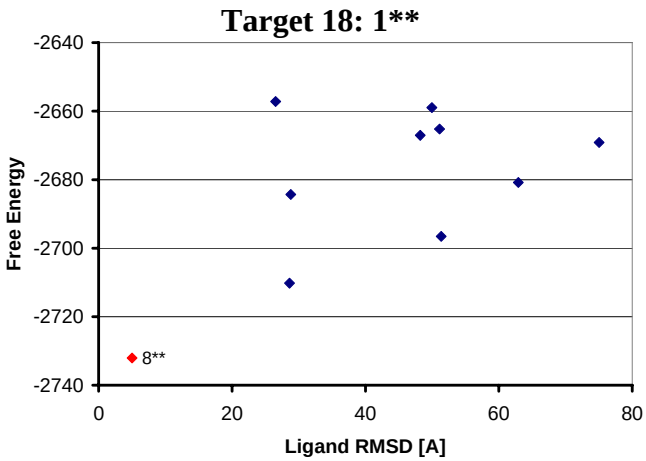
Target 18: 1**
Free Energy
-2640
-2660
-2680
-2700
-2720
-2740
0
20
40
60
80
8**
Ligand RMSD [A]

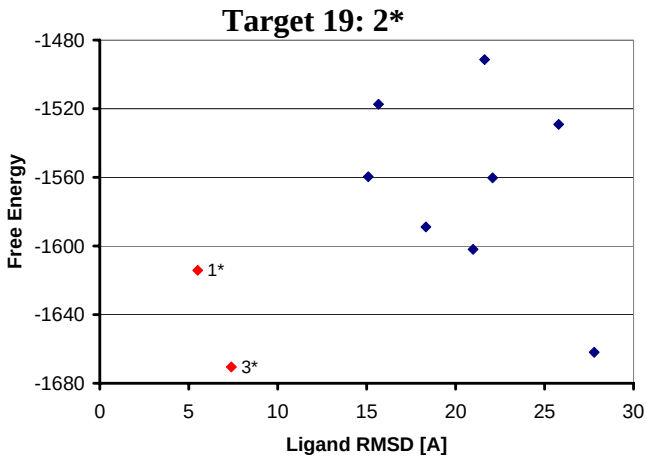
Target 19: 2*
Free Energy
-1480
-1520
-1560
-1600
-1640
-1680
0
5
10
15
20
25
30
1*
3*
Ligand RMSD [A]

FIGURE 3